Solid Electrolyte Interphase instability in operating Lithium-ion batteries unraveled by Enhanced-Raman Spectroscopy

Antonin Gajan,[1] Constance Lecourt,[1] Blanca Torres Bautista,[1] Laure Fillaud,[1] Julien Demeaux,[2] and Ivan T. Lucas,[1,3]

[1] Sorbonne Université, CNRS, Laboratoire LISE, 75000 Paris, France

[2] Saft, Corporate Research, 33074, Bordeaux, France

[3] Lead Contact

I- Experimental details

Electrochemical measurements – Electrochemical analyses were performed using either a Gamry Instrument (Reference 600+) or Origalys (OrigaFlex - OGF500) potentiostats in a two electrodes configuration. 1.0M $LiPF_6$ in EC/DEC=50/50 (v/v), 1.0M $LiPF_6$ in PC-$LiPF_6$ electrolyte mixtures were purchased from Sigma Aldrich, 1.2M $LiPF_6$ in EC/EMC=30/70 (v/v) were provided by Saft company. Tin foils electrodes were purchased from Alfa Aesar (Puratronic 99.998 %). Gold electrodes were obtained by evaporation on silicon substrate. Tin foil or thin film gold electrodes were assembled with a lithium foil and a polypropylene separator (Celgard 2325) in coin-cells (Hohsen Cop. ref 2032) filled with 60 µL of electrolyte and pressed using a MTI electrical crimper (MSK-160E). For *ex situ* Raman analysis, coin-cells were disassembled in an argon filled glove box and the tin or gold electrodes rinsed with DEC and placed in a sealed optical cell to prevent any air exposure during the Raman measurements.

Synthesis of bipyramid plasmon nanoamplifiers (SHINs)

<u>70-40 nm SHINs</u> (multistep protocols adapted from Liz-Marzan): Seeds of gold nanoparticles (GNPs) were first produced by mixing solutions of $HAuCl_4$ (10mL of 0.25 $mmol.L^{-1}$), citric acid (200 µL, 0.5 $mol.L^{-1}$), CTAC (10 mL, 0.05 $mol.L^{-1}$), reducer $NaBH_4$ solution (250 µL, 25 $mmol.L^{-1}$) and heating at 80°C for 90 minutes. Subsequent growth of the GNPs as bipyramids is achieved by adding to the seed solution, solutions of $HAuCl_4$ (500 µL, 10 $mmol.L^{-1}$), $AgNO_3$ (100 µL, 10 $mmol.L^{-1}$), HCl (200 µL, 1 $mol.L^{-1}$), ascorbic acid (80 µL, 100 $mmol.L^{-1}$) and CTAB (10 mL 0.1 $mol.L^{-1}$).

<u>140-40 nm SHINs</u> (multistep protocols adapted from Guyot-Sionnest): Seeds of gold nanoparticles (GNPs) were first produced by mixing solutions of $HAuCl_4$ (20mL of 0.125 $mmol.L^{-1}$), Trisodium citrate (500 µL, 10 $mmol.L^{-1}$) and $NaBH_4$ (30 µL, 100 mmol.L-1). The seeds solution were then then stored protected from dust and light for 30 days before use. Subsequent growth of the GNPs as bipyramids is achieved by mixing the seed solution (90 µL), solutions of $HAuCl_4$ (500 µL, 10 mmol.L-1), $AgNO_3$ (100 µL, 10 $mmol.L^{-1}$), HCl (200 µL, 1 $mol.L^{-1}$), ascorbic acid (80 µL, 100 $mmol.L^{-1}$) and CTAB (10 mL, 0.1 $mol.L^{-1}$).

The solution is then dialyzed to eliminate non-reacted precursors. A 3,5 KDalton dialysis membrane purchased from Spectrum Laboratories was filled with AuNPs colloidal solutions and placed in bi-distilled water changed each 24 hours during 3 days and protected from dust and light. Silica coating (adapted protocol from [1]) of the gold nanopyramids is then obtained by first vigorously stirring of 10 ml of the nanoparticle solutions to 2 mL of an aqueous solution of APTES (0.5 $mmol.L^{-1}$) during 30 minutes, and then adding 2 µL of a diluted sodium silicate solution (50 µL of 1,39 g/mL aqueous solution purchased from Sigma Aldrich in 8mL of distilled water), the pH of which had been previously adjusted to 10 using ion-exchange resin (Dovex 50Wx4). The solution is let to evolve during 5 days with slight stirring, out of the light. After centrifugation, the SHINs are dispersed in ethanol and kept at 5°C, also away from light. The following chemicals were used during the SHINs synthesis: Gold(III) chloride trihydrate ($HAuCl_4$, > 99.9%), Hexadecyltrimethylammonium chloride (CTAC, > 98%), Sodium borohydride ($NaBH_4$, > 98,5%), Hexadecyltrimethylammonium bromide (CTAB, > 98%), Silver nitrate ($AgNO_3$, > 99%), Silica sodium (reagent grade), (3-Aminopropyl)TrimethoxySilane (APTES, 97%) and Dowex 50WX4 hydrogen form were purchased from Sigma Aldrich.

SHINERS measurements - Raman measurements were performed using a Raman optical microscope (Horiba, LabRam Evolution HR800) equipped with 5 laser lines (473, 532, 594, 633, 785 nm) and a near-infrared sensitive CCD detector (Syncerity) and a scanning laser mode (DuoScan).

Ex situ SHINERS – SHINs dispersed in ethanol were deposited by drop casting on the substrate to be analyzed. Tin or gold electrodes decorated with SHINs were assembled in coin-cells, cycled in LIB electrolyte then disassembled, rinsed with solvent and placed in a sealed optical cell for their Raman analysis at 785 nm.

In situ SHINERS – Self-assembled monolayers on gold surfaces were obtained by prolonged contact of the gold surface with a solution of the azobenzene derivative (Prochimia Surfaces - HSC11O-azobenzene) in ethanol. A drop of LIB electrolyte was then added and covered using a glass coverslip.

Operando SHINERS – The superior cap of 2032 coin-cells (Hohsen Cop.) was drilled with a 3mm hole and then covered by a glass window (100µm thick cover-slip) affixed with epoxy glue. The lithium foil and the polypropylene separator were pierced in their middle of 5 mm and 3 mm diameter holes respectively and assembled with the SHIN-decorated electrode to be analyzed (tin foil or gold electrode) using a with 785 nm laser (0,9 mW, 3 seconds, 8 accumulations) and a 60x water dipping objective (Olympus LUMPLFLN60XW). The operando SHINERS measurements were carried out using the scanning mode of the laser (50 µm diameter circle) every 100mV (chronomamperometry step, 300 s) starting from the open circuit potential 2.8 V down to 100mV (first forward scan). The electrode was let to relax, polarized at 2,5V then a second potential scan was applied.

II- Optimization of SHINERS measurements for LIB applications

(***Electro)chemically inert SHINs*** – The electrochemical and chemical reactivity of SHINs and bare AuNPs assessed using electrochemical technique (cyclic voltammetry) and pyridine test to assess the effectiveness of the thin silica layer protection (homogeneity, pin-hole free), are presented in **Figure S1**:

- Bare or silica coated nanoparticles were deposited on a glassy carbon working electrode immersed in an H_2SO_4 aqueous electrolyte (0.1 mol/L). The potential of the working electrode was initially increased from the open circuit potential (OCP) to 1.4V / *SSE* (Saturated sulfate Electrode), at which a clear increase in current is observed, corresponding to the electrolyte oxidation. When gold particles are not (or only partially) covered with an insulating layer (black curve), gold oxides are also formed in parallel of the electrolyte oxidation above 0.7 V / *SSE*. During the potential backward scan, the cathodic peak associated to the reduction of these oxides appears at 0.45 V / *SSE*. In contrast, when the gold nanoparticles are coated with thin silica layer (red curve), no reduction peak is observed at 0.45 V / *SSE*, highlighting the absence of gold oxide formation and therefore the efficient electrochemical insulation of the synthesized SHINs.
- Pyridine which has a strong affinity for gold can be detected by Raman was briefly put in contact with bare or silica coated nanoparticles previously deposited on a silicon substrate. The Raman spectra in **Figure S1b** shows a band at 1010 cm^{-1} when the pyridine is adsorb on gold (pyridine/gold chemical bond vibration). Since this peak is no longer present after pyridine has been in contact with the SHINs, it can be concluded that the silica layer fully cover the gold NPs and is pin-hole free.

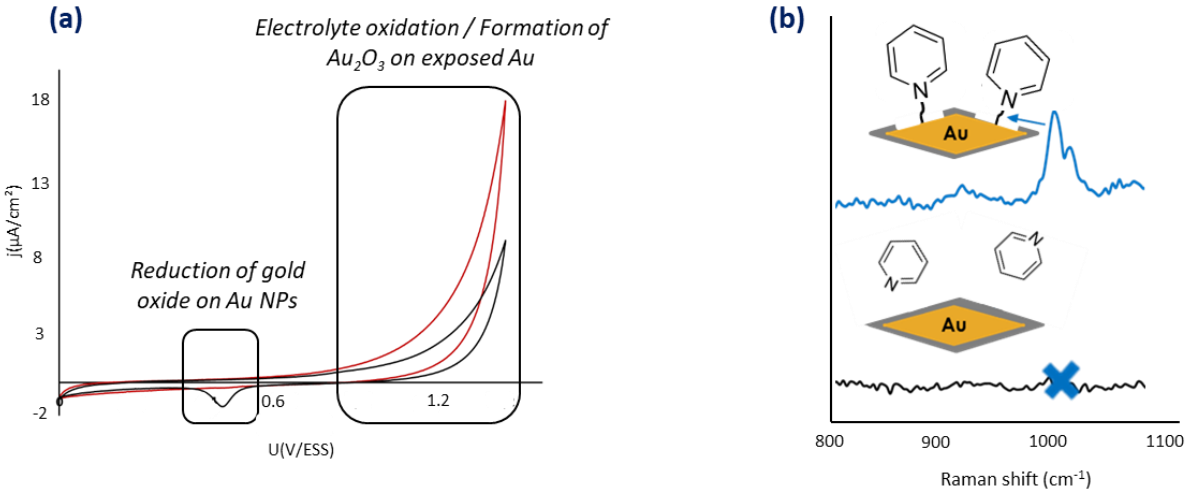

Figure S1. Test of the silica coating of the SHINs: (a) electrochemical response of bare (in black) and silica coated (in red) AuNPs - Cyclic voltammetry performed on a glassy carbon working electrode decorated with AuNPs / AuNPs@SiO_2. Mercury sulfate reference electrode in K_2SO_4 and a platinum wire as counter electrode were used in aqueous H_2SO_4 electrolyte concentrated to 0.1 mol/L. 0.1 V/s scan rate. **(b)** Raman spectra obtained on bare AuNPs (blue) and AuNPs@SiO_2 (black) deposited on mica and brought into contact with a pyridine solution.

Influence of SHINs on the LIB performances and interfacial processes – To assess both the impact of SHINs on the electrochemical activity/performances of LIB electrodes and on local enhancement of electrolyte degradation through photo-thermal effects upon laser irradiation, a series of tests was carried out.

Figure S2a shows the electrochemical response in the 2.7-0.5 V potential range (linear sweep) of a tin electrode in EC-DEC-$LiPF_6$ electrolyte (50/50 v/v, 1mol.L^{-1}) after deposition of bare and SiO_2-coated gold nanobipyramids respectively. The electrocatalytic properties of gold on tin for electrolyte degradation are clearly emphasized here, with charge associated to the electrochemical reduction process around 1.2V four time folded as compared to pristine tin electrode or tin decorated with Au@SiO_2 particles (SHINs). The very similar electrochemical response of tin with or without the presence of SHINs attests of the effective electrical insulation of the SHINs provided by the thin SiO_2 coating (5nm thickness).

The influence of laser irradiation on the electrolyte degradation in close vicinity of the SHINs (strong local plasmonic amplifiers) was also monitored at different laser power, time of exposure (photon dose) and reported in **figure S2b**. Upon irradiation at 785 nm, exposure time up to 80 seconds at laser power as low as 0.9 mm / µm² (laser spot dimension ~ 1µm) do not reveal any modification of the electrolyte composition while strong modification of its Raman signature is triggered at higher laser power (2.25 mW /µm²) at exposure time as short as 1 second. By continuous sweeping of the laser beam using two piezo-mirrors imprinting a 50 µm diameter circular pattern on the electrode surface decorated with SHINs, the photon dose per surface unit can be considerably reduced while maintaining high level of Raman signal, as demonstrated by the untouched electrolyte signature obtained even after 200 s of exposure at 4.5 mW.

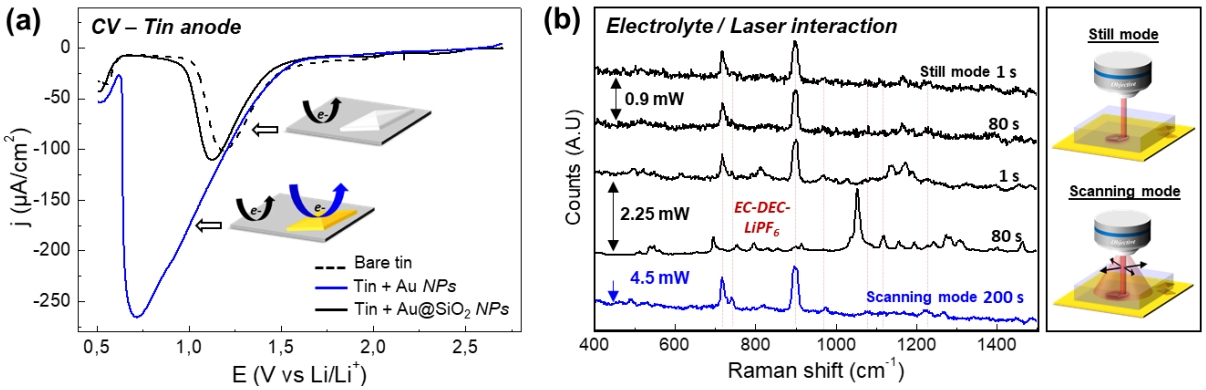

Figure S2: (a) Electrochemical responses of tin electrodes decorated with either bare gold nanoparticles (Au NPs: blue line) or silica coated gold nanoparticles (Au@SiO_2 SHINs, dark line) in 50/50 (v/v) EC/DEC, 1.0 M $LiPF_6$ electrolyte (linear sweep voltammetry between 2.8 V and 0.5 V vs Li/Li^+, beaker cell)). The chemical inertia of the synthetized SHINs (EC response similar to the one of bare tin shown in dotted line) contrasts with the apparent catalytic activity of the tin/gold NPs system on the reduction of the electrolyte. **(b)** Raman spectra of EC/DEC (50/50, v/v) 1.0 M $LiPF_6$ electrolyte (red dotted lines) on a SHIN decorated gold surface obtained at 785 nm for different laser power and time of exposure. While strong electrolyte composition changes are observed upon 2.25mW short beam exposure with still laser beam, no damage is observed using a scanning laser beam (50µm diameter disc pattern) even at long exposure time and laser power as high as 4.5mW.

Raman signal enhancement at extreme polarization –A gold electrode functionalized self-assembled monolayer of a thioazobenzene derivative was decorated with spherical SHINs of 90 nm diameter to evaluate the possible variation/damping of the Raman signal enhancement over wide ranges of electrochemical potentials. The electrode was placed in a three electrode cell (counter electrode: gold wire, reference: silver wire) filled with a solution of tetrabutylammonium hexafluorophosphate in acetonitrile and polarized between [-2V; +2V] vs E(Ag/Ag$^+$) which corresponds to the stability range of this electrolyte. Raman spectra of the azobenzene derivative (**Figure S3**) collected *operando* do not show any damping in the band intensity over the scanned potential range.

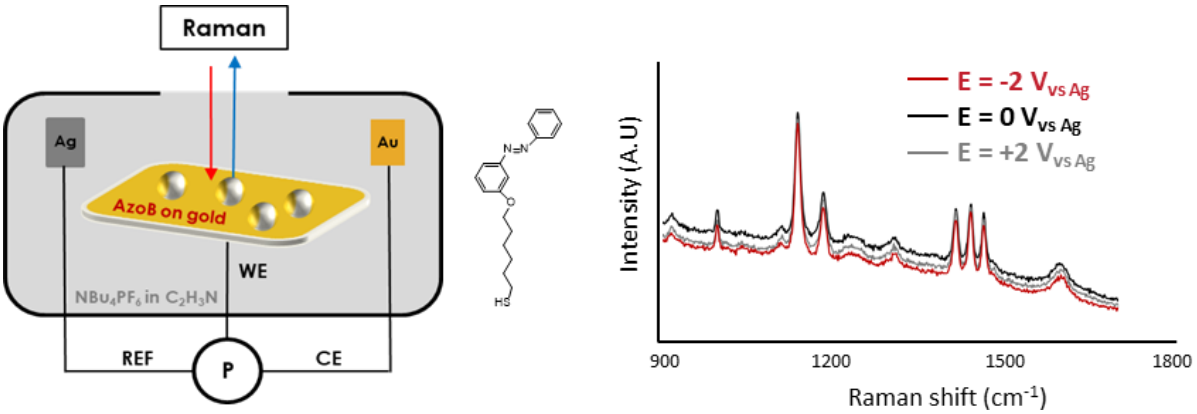

Figure S3. Operando SHINERS at extreme polarization [-2;+2V] on thioazobenzene derivative functionalized gold substrate in $TBAPF_6$ (0.5M) acetonitrile electrolyte. Raman measurement were carried out on the functionalized gold electrode decorated with spherical SHINs of 90 nm diameter (λ_{exc} = 785 nm, P= 90 µW, t = 5 seconds, 5 accumulations).

Design of a Coin-cell like operando Raman cell – Most operando studies, i.e. microscopies, (spectroscopies, gravimetry) are carried out in simple 2 or 3 electrodes cells which the design is dictated by the constrains of the analytical techniques. Large volume of electrolyte, possible air contamination and non-optimized distribution of current lines within such cell designs (positioning of counter and reference electrodes) may affect the quality of the analysis. This is particularly true for high-energy storage systems like Lithium-ion batteries in which high current densities can be associated to large ohmic drop (contact and electrolyte ohmic resistance), and in which the "filming" properties of the electrodes (passive layer formation : SEI, CEI) critically depends on both the volume and quality of the electrolyte (moisture and oxygen free). **Figure S4a&b** depict the electrochemical behavior of a tin foil electrode within the 2.8 – 0.5 V potential range (versus lithium) in two home-made spectroelectrochemical cells filled with respectively, 1mL (standard or beaker cell) and 60µL (pressurized electrode-sandwich assembled as a "coin-cell") of EC-EMC-$LiPF_6$ electrolyte mixture. While both systems show similar early stages of lithiation (E < 0.6 V) and delithiation (0.7 < E < 1 V), the irreversible reduction current peak spanning from 1V to 1.5 V which is associated to the SEI formation on tin, shows strong intensity difference between the two configurations. By contrast with tin anodes in beaker cell that exhibit partial SEI dissolution due to the larger volume of electrolyte, tin surface passivation is achieved after the first cyclic voltammetry (CV) cycle in a coin cell. Note also that a smaller reduction peak is also observed as potential as high as 2.4V (early stages of formation of the SEI) only for the beaker-cell configuration. The spectroelectrochemical coin-cell is therefore used over the entire study to minimize possible design-related interfacial processes and misleading associated spectral information.

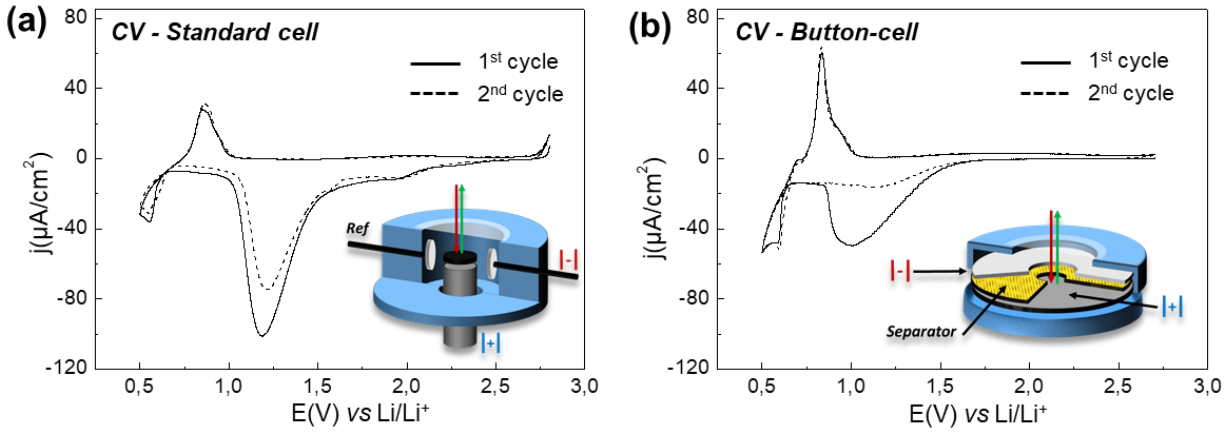

Figure S4. Electrochemical response (cyclic voltammetry) of a tin electrode in spectroelectrochemical cells filled with EC-EMC $LiPF_6$ electrolyte (counter electrode: lithium foil). The depicted spectroelectrochemical cell design (volume of electrolyte, current line), i.e. **(a)** standard cell (beaker cell) and **(b)** coin-cell also called "button-cell", largely influences the passivation properties of the electrode.

SHINERS efficiency in LIB electrolytes **–** Carbonate-based LIB electrolytes display fluorescence properties which translates into large background on Raman spectra (**Fig. S5a**) and difficulties to isolate the scattered signal contribution containing the Raman information. To circumvent this limitation, near-infrared excitation 785 nm can be used, or alternatively Kerr gate Raman spectroscopy recently proposed by Hardwick et al [2].

To achieve high SHINERS enhancement factors with near-infrared excitation, large spherical gold nanoparticles (120 nm Au@SiO_2 SHINs) with raspberry shape were first synthesized, but their performance turned out to be outmatched by the one of anisotropic gold nano-bipyramids (length and width: 140 nm and 40 nm, or 70 nm and 40nm).

Figure S5b shows the UV-Vis spectra of the first synthetized colloidal solution, with two main absorbance maxima, one around 950 and 580 nm associated to gold nano bipyramids and spherical/oblong objects respectively. This latter population, observed together with bipyramids by electron microscopy (SEM) in the insert **figure S5b** (NP suspension drop-casted on a gold substrate), is inherent to the synthesis method and can be partially removed after centrifugations.

To demonstrate the efficiency of the produced SHINs to extract the chemical signature of thin layers in contact with carbonate based electrolyte, non-Raman resonate self-assembled monolayers (SAM) of a thio-Azobenzene derivative on gold substrates were analyzed *in situ* using different Raman probes (532, 633 and 785 nm). **Figure S5c** confirms that no SAM signature can be observed by standard far-field microRaman but that strong signal can be extracted both *ex situ* and *in situ* in LIB electrolyte using bipy-SHINs. The clearest SAM Raman signatures (blue bands), free of fluorescence background, were observed amid the bands of the electrolyte (black bands) using 785 nm excitation at minimal collection time and laser power (power 0.9mW; acq. time 1s; 10 accumulations), paving the way to *operando* characterization of SEI using near-infrared excitation. Note that the enhancement factor cannot be determined accurately as the number of SHINs (random distribution of NPs drop casted on the electrode, formation of agglomerates) in interaction with the laser beam or the substrate upon measurements is not assessable.

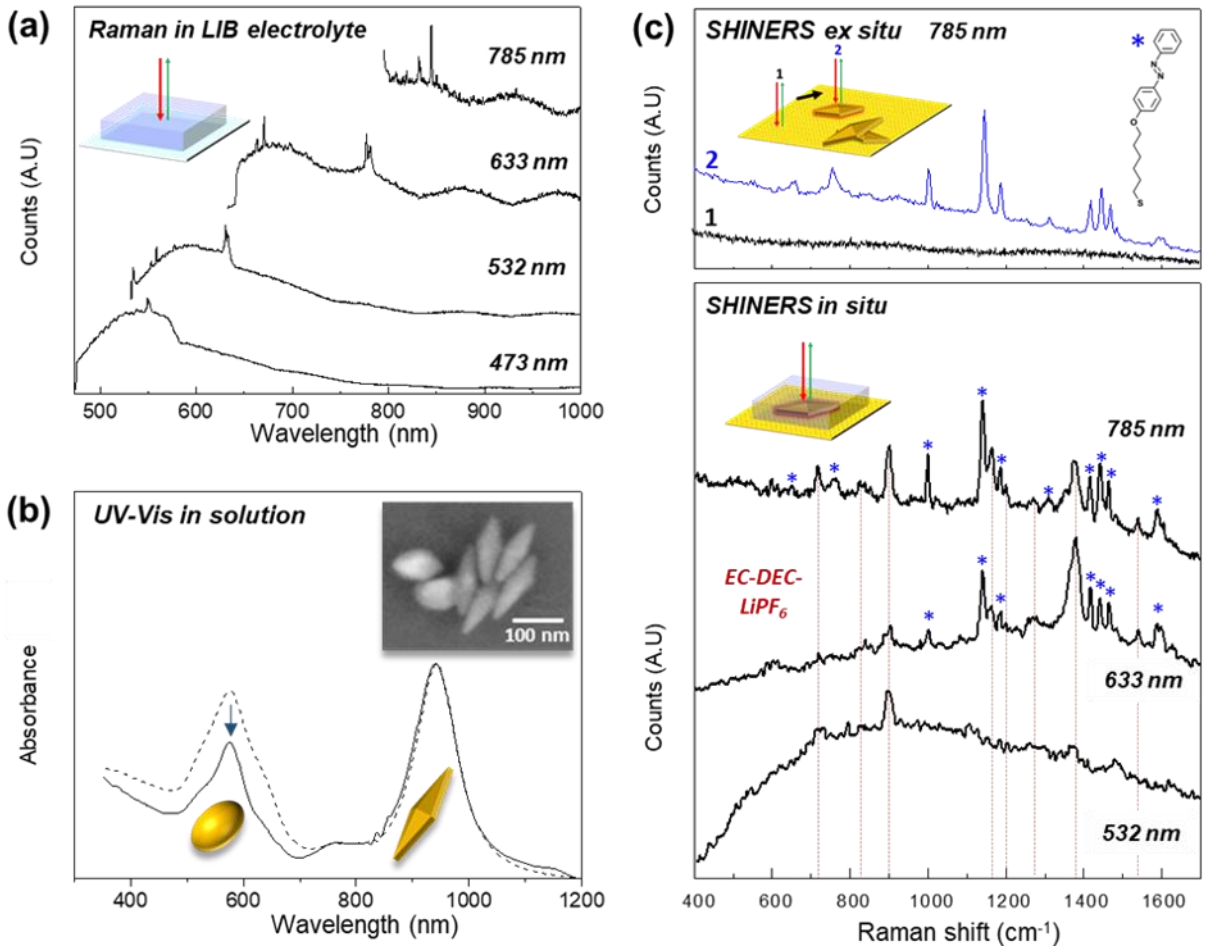

Figure S5: (a) Raman spectra of EC-DEC $LiPF_6$ electrolyte used in LIB highlighting the influence of the Raman probe on the Raman signal over fluorescence background ratio. Measurements using a near-infrared excitation (i.e. 785 nm) allow minimizing the strong fluorescence background of the electrolyte observed for other excitations and recovery of the electrolyte Raman signature (b) UV-vis spectra of colloidal suspensions of anisotropic gold nanoparticles (plasmonic nano amplifiers) designed for near-infrared SHINERS. UV-vis spectra and the SEM micrograph in the insert show two populations with absorbance properties in the near-infrared (λ_{abs}: 950nm, 140nm long bipyramid particles) and orange spectral domain (λ_{abs}: 580nm, oblong shape particles) respectively, the ratio of which can be increased after centrifugation. (c) Anisotropic particles once covered with silica shell proved to successfully extract at 785 nm excitation the Raman signature of a non-Raman resonant molecular monolayer (azobenzene derivative) self-assembled on a gold substrate. Similar signatures (blue stars) could be extracted *in situ* within a thick layer of LIB electrolyte (red dotted lines) deposited on the SAM functionalized gold substrate, with minimum fluorescence background.

III- Operando SHINERS measurements in LIB systems

Visualization of the SHIN deposits and of the SEI **– Figure S6** shows images captured from the optical microscope of the Raman spectrometer using a x60 objective before and after the polarization of SHIN decorated gold electrode in LIB electrolyte. The images reveal the morphology of SHIN agglomerates (hotspots) formed by drop casting of the SHIN colloidal solution (dispersion in EtOH) on a pristine gold electrode and the roughening due to SEI formation after cycling in LIB electrolyte.

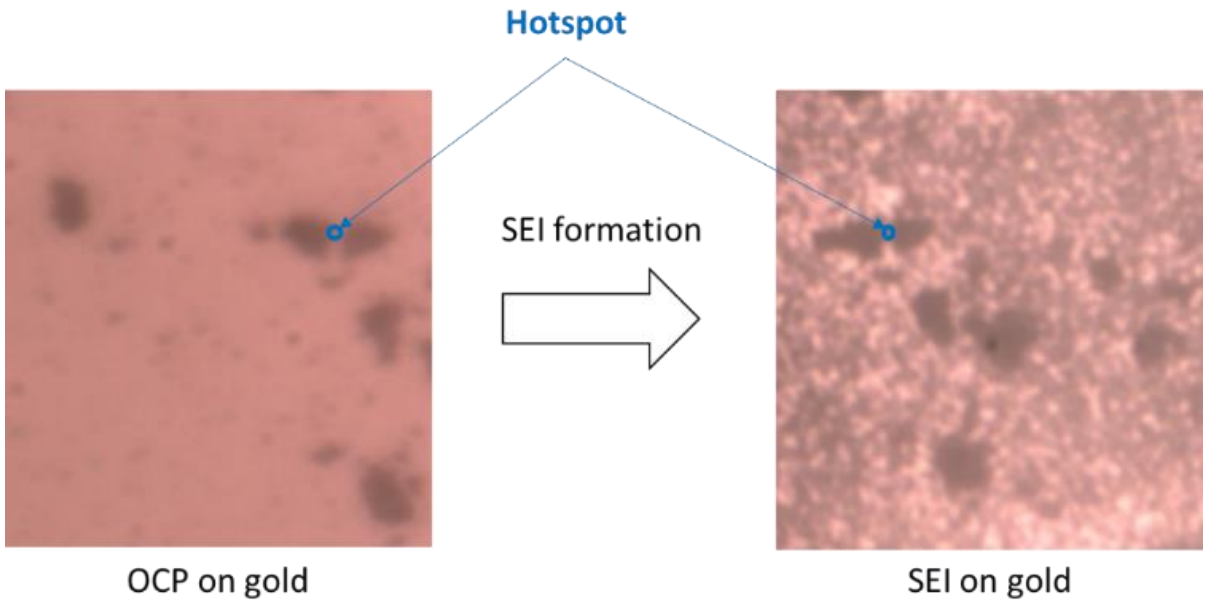

Figure S6. Optical microscope image of the Raman spectrometer before and after reduction of the electrolyte EC-DEC-$LiPF_6$ on gold electrode. The laser remains focused on the hotspot noted by a blue circle on the image across the whole SHINERS measurement (corresponding results presented in **Figure S7**).

***Operando* SHINERS on gold in EC-DEC $LiPF_6$ -** *Operando* SHINERS measurement results on gold in EC/DEC=50/50 (v/v), 1.0 M $LiPF_6$ electrolyte are given in **Figure S7**.

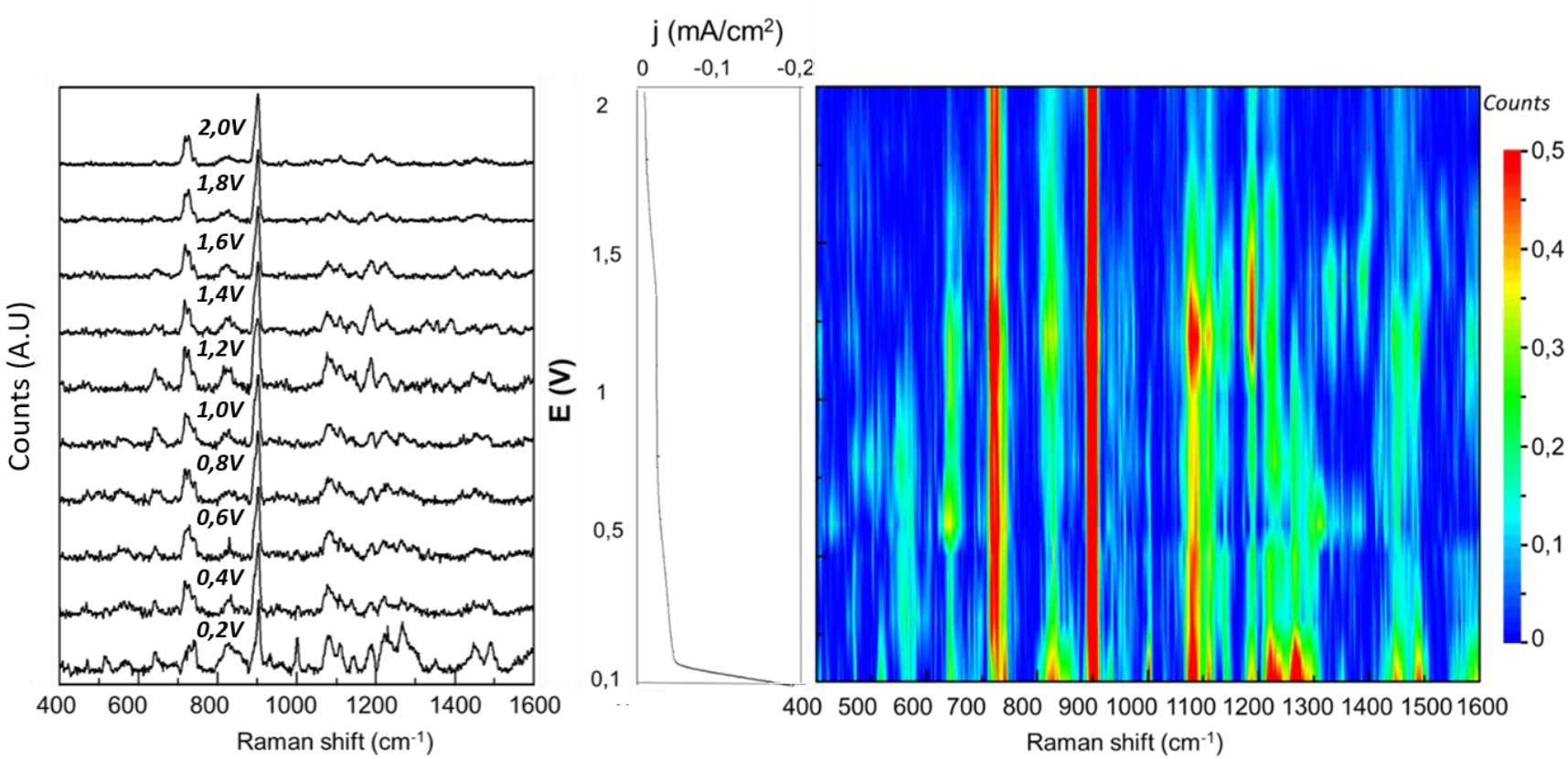

Figure S7. Operando SHINERS on gold electrode polarized in EC/DEC=50/50 (v/v), 1.0 M $LiPF_6$ electrolyte. Raman spectra were collected at 785 nm (laser power 0.9mW, t_{acq} = 3 seconds, 8 accumulations) every 100mV (upon a 0.33 mV/s Linear swap voltammetry) from the OCP (2.8V) down to 0.1V vs Li/Li^+ (first forward scan). Spectra were baseline subtracted and normalized on the 900 cm^{-1} band intensity (electrolyte).The linear sweep voltammogram obtained during the experiment between 2.0 V and 0.1 V (versus lithium) at 0.33 V/s is also given. The 2D color map representing the Raman band intensity as a function of the applied potential allows to appreciate the dynamics of composition of the tin electrode / electrolyte interface. Note the absence on gold of the band at 501 cm^{-1} attributed to DEDOHC.

Operando SHINERS on tin in EC-DEC $LiPF_6$ – The full set of data of ***o***perando SHINERS (Raman spectra from 2.5V to 0.1V vs Li/Li^+) obtained on tin in EC/DEC=50/50 (v/v) 1.0 M $LiPF_6$ electrolyte is given in **Figure S8**.

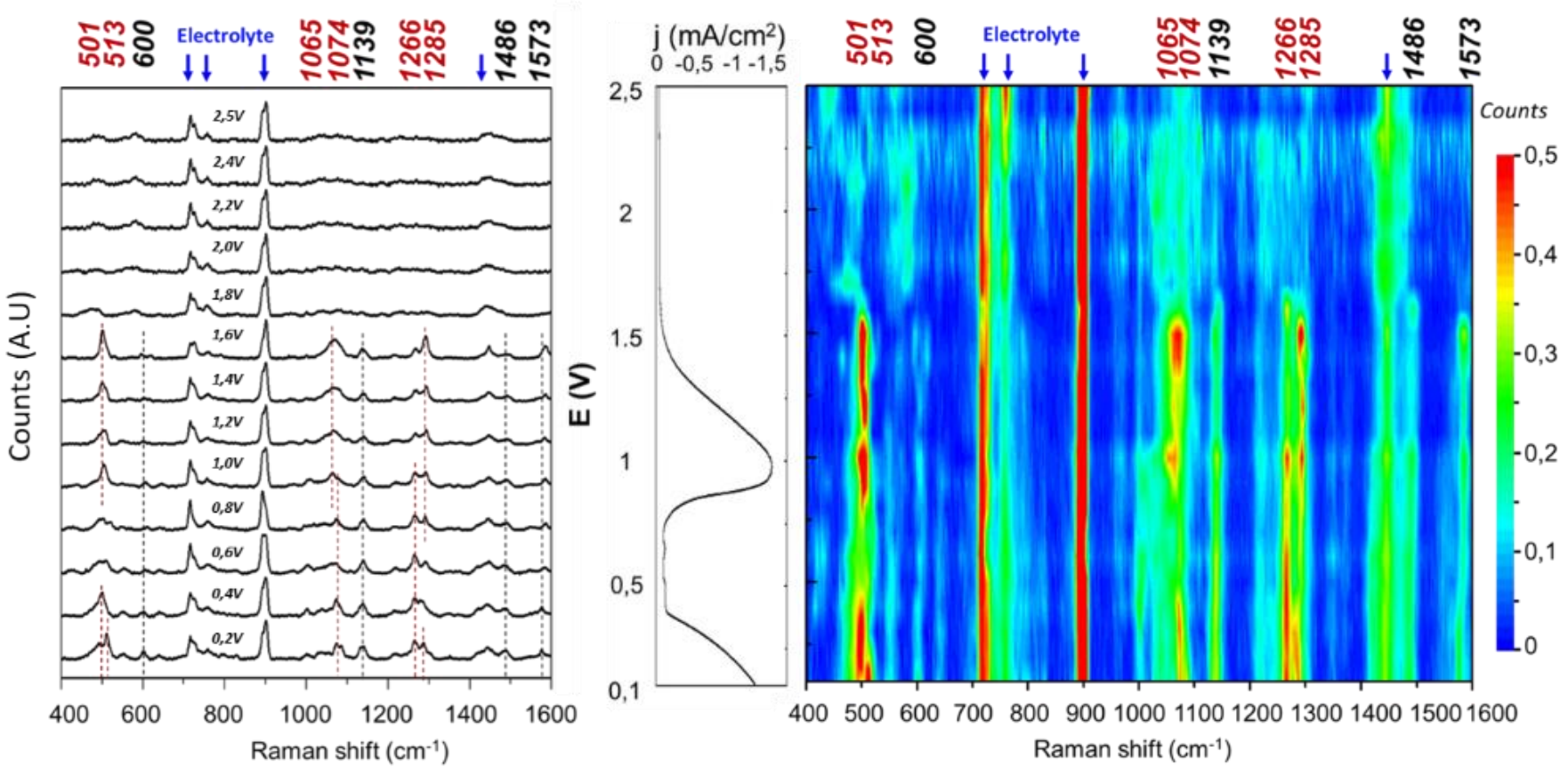

Figure S8. Operando SHINERS on tin electrode polarized in EC/DEC=50/50 (v/v), 1.0 M $LiPF_6$ electrolyte. Raman spectra were collected at 785 nm (laser power 0.9 mW, t_{acq} = 3 seconds, 8 accumulations) every 100mV steps (after 5min chronoamperometry) from 2.5V down to 0.1V vs Li/Li^+ (first forward scan). Spectra were baseline subtracted and normalized on the 900 cm^{-1} band intensity (electrolyte). Dotted lines correspond to new Raman bands appearing during polarization (only bands marked with red dotted lines were attributed). A linear sweep voltammogram obtained on this same system between 2.5 V and 0.1 V (versus lithium) at 0.33 V/s is given to guide the eyes. The 2D color map representing the Raman band intensity as a function of the applied potential allows to appreciate the dynamics of composition of the tin electrode /electrolyte interface.

Reproducibility of operando SHINERS on tin in EC-DEC LiPF$_6$ – SHINERS measurement on tin electrode in EC/DEC=50/50 (v/v), 1.0 M LiPF$_6$ electrolyte were repeated 4 times. The Raman spectra collected at the last polarization step (after 100mV vs Li/Li$^+$) in the four different experiments are presented in **Figure S9**.

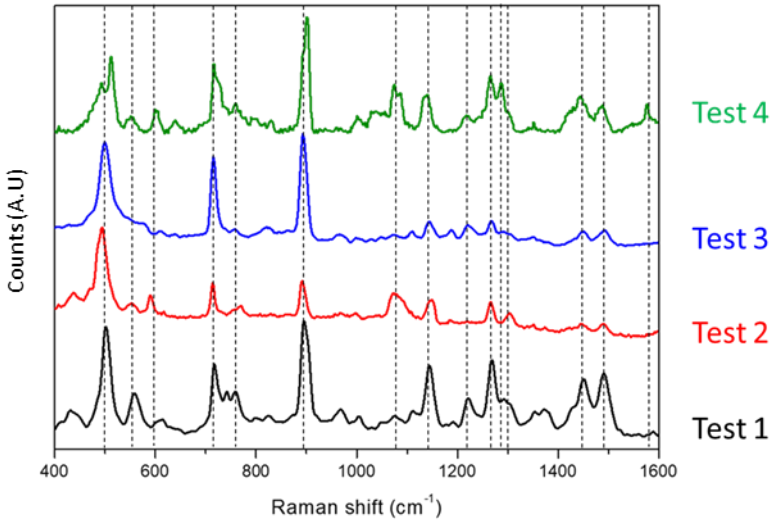

Figure S9. Raman spectra (SHINERS) obtained on 4 distinct experiments using the same exact conditions (Sn vs Li in EC/DEC=50/50 (v/v), 1.0 M LiPF$_6$ electrolyte, after polarization at 100mV.

Operando SHINERS on tin in EC-EMC LiPF$_6$ - Operando SHINERS measurement has also been performed on a tin electrode in EC/EMC=30/70 (v/v), 1.2 M LiPF$_6$ electrolyte. Results presented in **Figure S10** highlight the systematic loss of Raman signal at potential lower than 1V vs Li/Li$^+$. The signal is not recovered while scanning back at higher potential, highlighting the stability of the SEI. The SEM micrograph image presented in **Figure S10c** was realized on the cycled tin electrode after disassembling of the cell and rinsing of the electrode. In contrast with the images presented in **Figure 2** in the main manuscript showing the SHINs floating on the SEI (tin, EC-DEC LiPF$_6$) the SHINs appear here like embedded in a thick SEI layer which could explain the loss of signal in EC-EMC LiPF$_6$ electrolyte. This loss of the signal enhancement properties of the SHINs is currently under investigation.

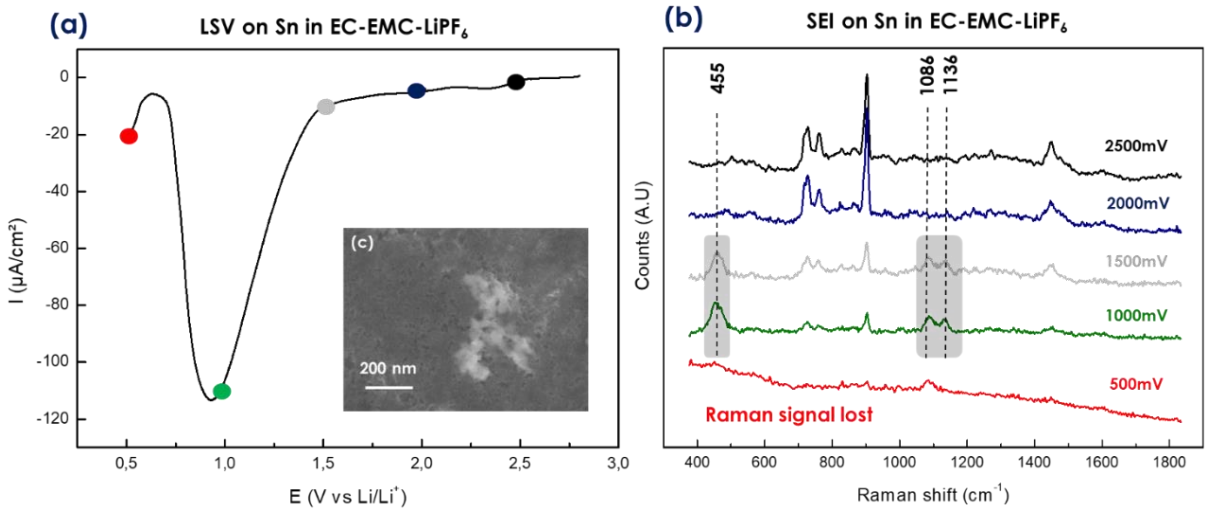

Figure S10: Operando SHINERS on tin electrode in EC/EMC=30/70 (v/v), 1.2 M LiPF$_6$ electrolyte. **(a)** Electrochemical response (Linear Sweep Voltammetry LSV 1 mV/s), **(b)** Raman spectra were collected at 785 nm (laser power 0.9 mW, t_{acq} = 3 seconds, 8 accumulations) every 500mV from the OCP (2.8V) down to 0.5V vs Li/Li$^+$ (first forward scan). Spectra were normalized on the 900 cm^{-1} band intensity

(electrolyte). SEM images of the SHINs decorated tin electrode after the experiment (disassembling of the cell in glove box and electrode rinsed with EMC) are presented in (c).

IV - Raman spectra assignment

Synthesis protocols and characterization of synthetic SEI organic components

LEC: Lithium ethyl carbonate:

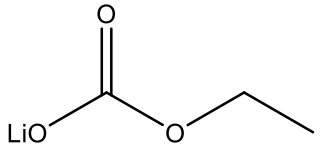

R = 76 %

Molecular Weight: 96,01

➔ ***Synthesis protocol (adapted from [3]):***

Lithium ethoxide (4.8 mmol, 250 mg) was dissolved under inert atmosphere in absolute ethanol (50mL). After 15 minutes of vigorous stirring under argon, the solution was bubbled with dry CO_2 gas at room temperature for 3 hours. The solvent was removed under vacuum to afford white powder of lithium ethyl carbonate. (210 mg, 76%)

➔ ***Characterization:***

^{1}H NMR DMSO-d_6 400 MHz: δ (ppm) 3.70 (m, 2H, –O–**CH_2**–CH_3), 1.04 (t, *J* = 7.1 Hz, 3H, –O–CH_2–**CH_3**)

^{13}C NMR DMSO-d_6 400 MHz: δ (ppm) 156.17 (LiO–**C**(=O) –O–), 58.70 (–O–**CH_2**–CH_3), 15.64 (–O–CH_2–**CH_3**)

^{7}Li NMR DMSO-d_6 400 MHz: δ (ppm) -0.97

LMC: Lithium methyl carbonate:

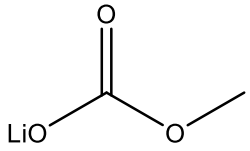

R = 66 %

Molecular Weight: 81,98

-

➔ ***Synthesis protocol (adapted from [3]):***

Anhydrous methanol (20 mL) is added in a pre-dried assembly under inert atmosphere. The reaction mixture is cooled to - 40°C and BuLi (2.5M in hexane, 40 mmol, 16 mL) is added. The reaction was warmed to room temperature and further stirred for 30 minutes. Dry CO_2 gas was bubbled through the solution for 2 hours at room temperature. The solvents was removed under vacuum, leaving a white powder that was further rinsed with anhydrous diethyl ether. The resulting white powder was dried under vacuum overnight to afford LMC. (260 mg, 66%)

➔ ***Characterization:***

^{1}H NMR DMSO-d_6 400 MHz: δ (ppm) 3.26 (s, 3H, –O–**CH_3**)

^{13}C NMR DMSO-d_6 400 MHz: δ (ppm) 156.05 (LiO–**C**(=O) –O–), 51.16 (–O–**CH_3**)

^{7}Li NMR DMSO-d_6 400 MHz: δ (ppm) -1.10

LEMC: Lithium ethylene mono-carbonate

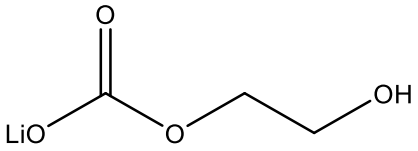

R = 59 %

Molecular Weight: 112,01

➔ ***Synthesis protocol (adapted from [4]):***

Anhydrous ethylene glycol (EG) (0.36 mol, 22.26 g, 20 mL) is added in a pre-dried assembly under inert atmosphere. The reaction mixture is cooled to -40°C and BuLi (2.5M in hexane, 0.11 eq, 40 mmol, 16mL) is added. After returning to room temperature, the mixture is kept under stirring for 30 minutes. Hexane was evaporated under vacuum and a suspension of lithium ethylene glycol (LiEG) in EG is obtained. Dry CO_2 is bubbled into the reaction mixture and after two hours the mixture becomes clear. Anhydrous pyridine (50 mL) is then added and the reaction mixture is kept under agitation and argon for two days. A white precipitate appears, which was collected through centrifugation, rinsed with anhydrous DMF and anhydrous diethyl ether, and further dried under vacuum overnight to afford lithium ethylene mono carbonate (LEMC) (2.64 g, 59%).

➔ ***Characterization:***

^{1}H NMR DMSO-d_6 400 MHz: δ (ppm) 3.69 (t, *J* = 5.5 Hz, 2H, –O–**CH_2**–CH_2–OH), 3.43 (t, *J* = 5.5 Hz, 2H, –O–CH_2–**CH_2**–OH), 4.97 (s, 1H, –O–CH_2–CH_2–**OH**)

^{13}C NMR DMSO-d_6 400 MHz: δ (ppm) 156.71 (LiO–**C**(=O)–O–), 65.67 (–O–**CH_2–CH_2**–O–), 61.09 (–O–**CH_2–CH_2**–O–)

^{7}Li NMR DMSO-d_6 400 MHz: δ (ppm) -1.24

LEDC: Lithium ethylene di-carbonate

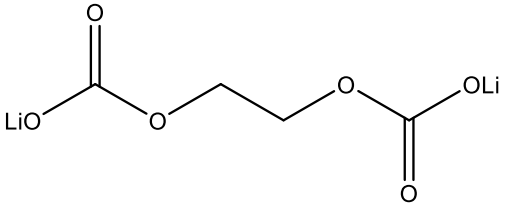

R = 25%

Molecular Weight: 161,95

➔ ***Synthesis protocol (adapted from [4]):***

Lithium tert-butoxide (120 mg, 1.5 mmol) is added to a solution of LEMC (112 mg, 1.0 mmol) dissolved in anhydrous DMSO (freshly distilled, 5 ml). The solution is then stirred for 30 min. Dry CO_2 is bubbled into the reaction mixture during 30 minutes. 1 mL of anhydrous diethyl ether (freshly distilled) is added to the solution. The reaction mixture is kept under vacuum overnight at 40°C to evaporate the solvent yielding a white powder of lithium ethylene di-carbonate (LEDC.2DMSO) (40 mg, 25%).

➔ ***Characterization:***

^{1}H NMR DMSO-d_6 400 MHz: δ (ppm) 3.38 (s), 2.54 (s)

^{13}C NMR DMSO-d_6 400 MHz: δ (ppm) 63.11, 62.38

^{7}Li NMR DMSO-d_6 400 MHz: δ (ppm) -1.33

LiO^{t}Bu: Lithium tert-butoxide

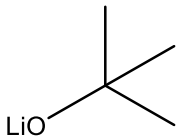

R = 86 %

Molecular Weight: 80,06

➔ ***Synthesis protocol (taken from [4]):***

To a solution of tert-butyl alcohol (54 mmol, 4.0 g) dissolved in anhydrous diethyl ether (20 mL) at -40°C, n-BuLi (2.5 M in hexane, 54 mmol, 21.6 mL) was added dropwise. The reaction was warmed to room temperature and further stirred for 30 minutes. Solvent was remove under vacuum overnight to yield a white powder of lithium tert-butoxide (3.72 g, 86 %).

➔ ***Characterization:***

^{1}H NMR $CDCl_3$ 400 MHz: δ (ppm) 1.16 (s, 9H, –**CH_3**)

^{13}C NMR $CDCl_3$ 400 MHz: δ (ppm) 35.47 (–**CH_3**), 31.40 (LiO–**C**–$(CH_3)_3$

LPDC: Lithium propylene di-carbonate

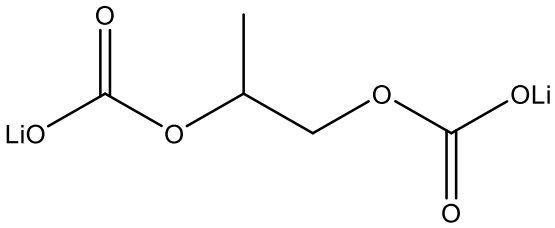

R = 26 %

Molecular Weight: 175,98

➔ ***Synthesis protocol (adapted from [5]):***

Propane-1,2-diol (13.6 mmol, 1.036 g, 1 mL) was added dropwise, under vehement stirring and a dry argon stream, to a stoichiometric amount of BuLi (2.5M in hexane, 27.2 mmol, 10.8 mL) solution diluted by anhydrous diethyl ether (10 mL). The resultant dialkoxides were then isolated, dried under vacuum, and then suspended in dry acetonitrile for carbonization. With vehement stirring, dry CO_2 gas was bubbled into the suspension. White crystals appears, which were dried under vacuum overnight to afford lithium 1,2-propylene di carbonate. (0.580 g, 26 %)

➔ ***Characterization:***

^{1}H NMR DMSO-d_6 400 MHz: δ (ppm) 3.68 (tq, *J* = 10.7, 6.5, 5.5 Hz, 1H, –O–**CH**(CH_3)–CH_2–O–), 3.32 (m, 2H, –O–CH(CH_3)–**CH_2**–O–), 1.04 (d, *J* = 6.3 Hz, 3H, –O–CH(**CH_3**) –CH_2–O–)

^{13}C NMR DMSO-d_6 400 MHz: δ (ppm) 68.73-68.47 (–O–**CH**(CH_3)–**CH_2**–O–), 19.51 (–O–CH(**CH_3**)–CH_2–O–)

^{7}Li NMR DMSO-d_6 400 MHz: δ (ppm) -1.28

In situ and ex situ SHINERS response - SHINERS experiment have been performed on two different anode materials (on gold and tin electrode) *ex situ* and compared to *in situ* results on tin. **Figure S11** shows a comparison of the different SEI Raman spectra (after 100mV polarization in EC/DEC=50/50 (v/v), 1.0 M $LiPF_6$ electrolyte) and the comparison with the signature of the electrolyte (the Raman shift associated to each Raman band is given for the sake of clarity). While some of the Raman bands have been successfully attributed to specific chemical compounds, many remains unattributed and further efforts will need to be done in future studies. Differences observed between the three systems can be explained by the heterogeneity of the SEI, the difference of surface reactivity of different metals and by the rinsing of the electrode for *ex situ* measurement (the excellent Raman signal collection efficiency for *ex situ* measurement can explain the larger number of bands as compared to in situ measurements).

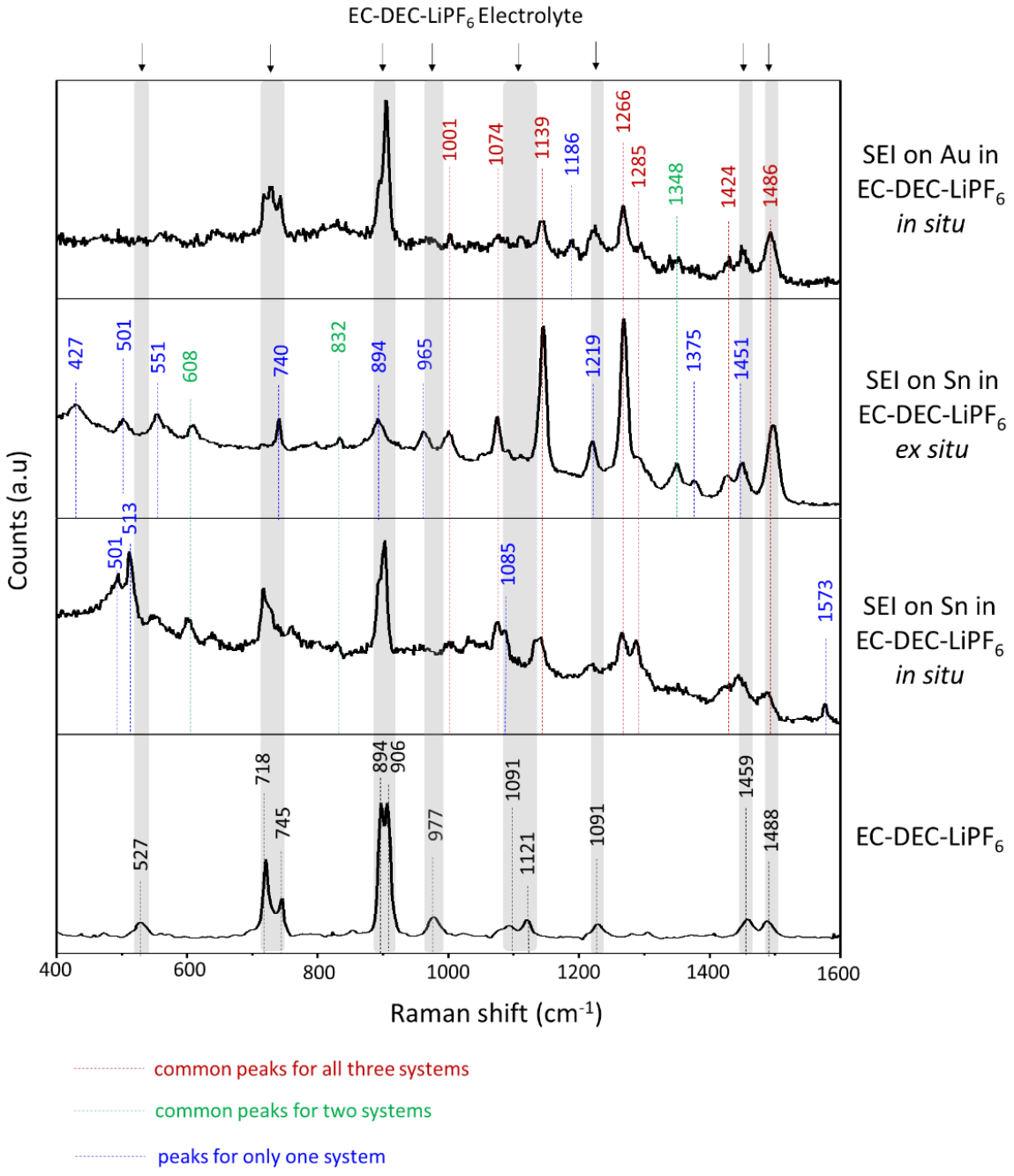

Figure S11: Comparison of the Raman spectra obtained on gold electrode in situ at 100mV, on tin electrode at 100mV and ex situ on tin electrode after a 100mV polarization. All three experiments were performed in similar conditions in EC/DEC=50/50 (v/v), 1.0 M $LiPF_6$ electrolyte. Raman spectra were all collected at 785 nm.

Raman signature of reference compounds – The recurrent problem of spectral assignment must be addressed by establishing a databank of Raman signatures of various SEI organic components possibly formed in EC/DEC LiPF6 electrolyte (presented in **Figure S12a, b, c**). We propose here a first Raman spectra library of SEI components which could be of great use to the analytical community. Note that these spectra were collected at 785 nm excitation. **The strong fluorescence background observed experimentally with 532nm excitation for the reference compounds LEMC, LEC, LMC and LPDC also justifies the use of near-infrared excitation**. Some compounds were mixed with aliquots of EC-DEC $LiPF_6$ electrolyte to assess possible solvation effects on the Raman band positions.

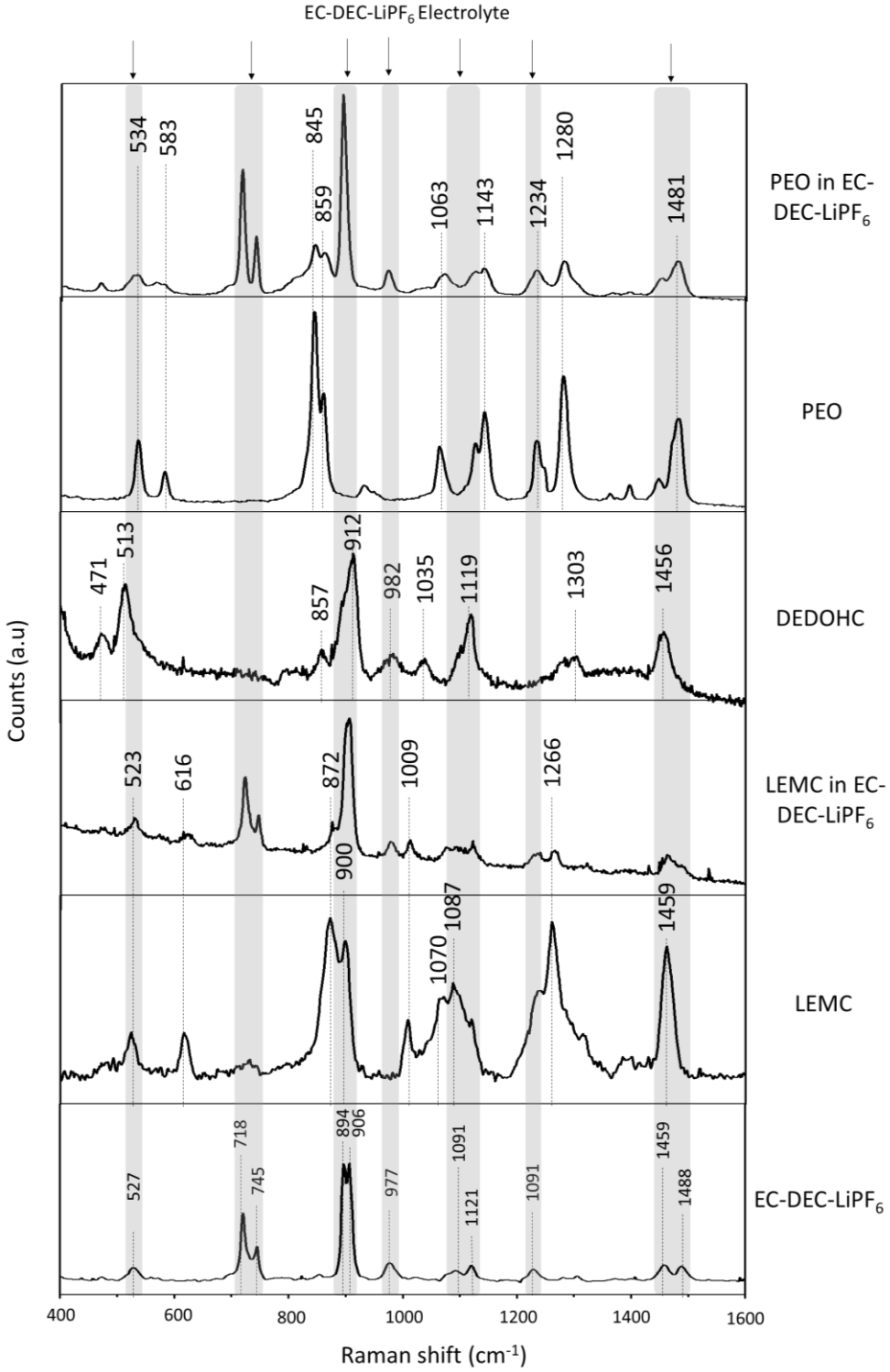

Figure S12a. Raman spectra of different possible SEI components. All measurement were performed under Argon atmosphere at 785 nm. LEMC and PEO powders were collected both alone or soaked with EC/DEC=50/50 (v/v), 1.0 M $LiPF_6$ electrolyte.

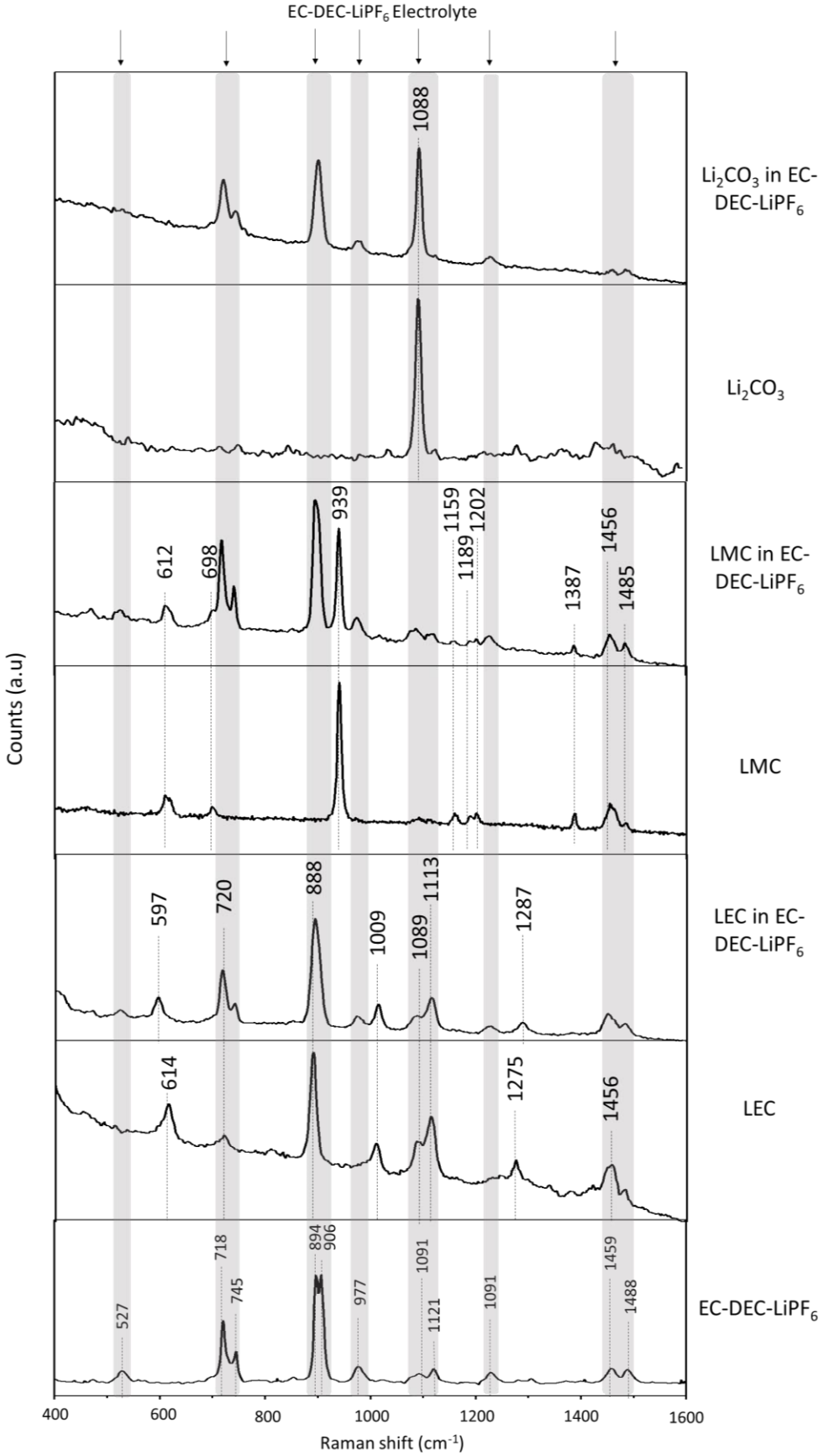

Figure S12b: Raman spectra of different possible SEI components. All measurement were performed under Argon atmosphere at 785 nm. LEC, LMC and Li_2CO_3 powders were collected both alone and mixed with EC/DEC=50/50 (v/v), 1.0 M $LiPF_6$ electrolyte.

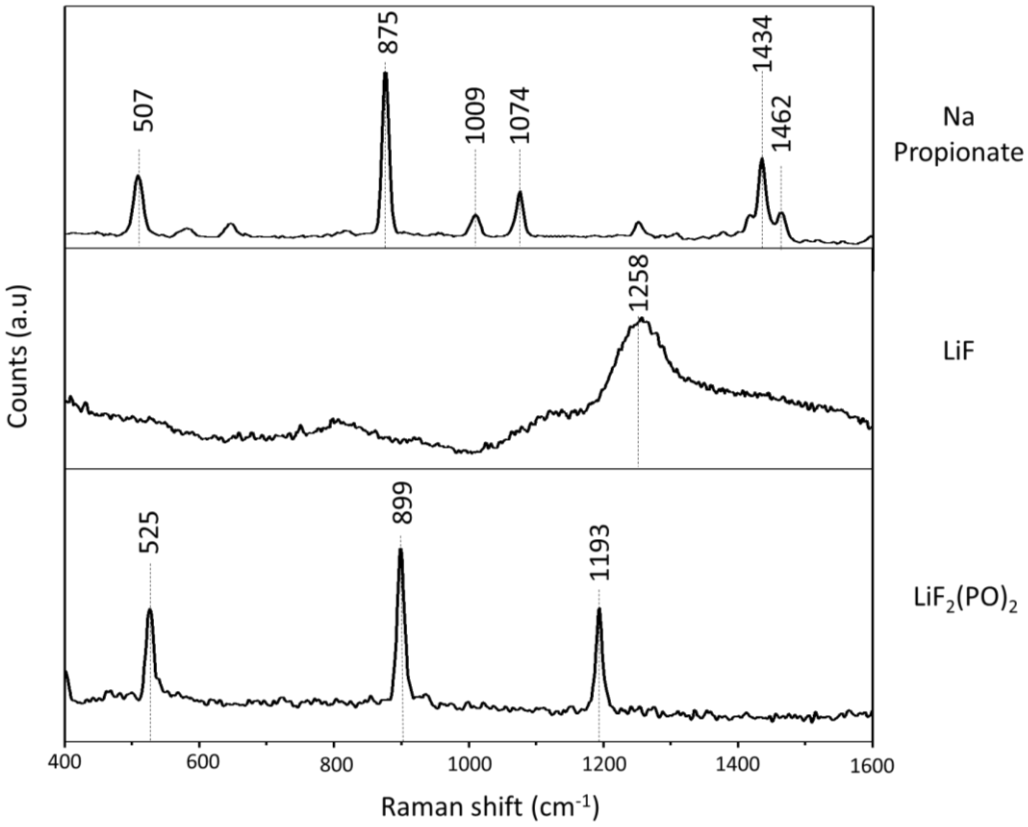

Figure S12c: Raman spectra of different possible SEI inorganic components. All measurement were performed under Argon atmosphere at 785 nm.

SEI on tin/gold in EC-DEC $LiPF_6$ electrolyte vs DEDOHC – Comparison of the Raman spectra of the SEIs with the one of DEDOHC often reported as a SEI component (**Figure S13**), shows the bands matching of the liquid DEDOHC with band of the SEI obtained *in situ* on tin electrode. No DEDOHC is found neither *ex situ* on tin (DEC rinsing of the electrode and DEDOHC soluble in DEC) nor *in situ* on gold (DEDOHC formation on tin result from a catalytic process involving surface tin oxides). Thru this comparison, the bands of the SEI at 501 and 513 cm^{-1} was assigned to DEDOHC.

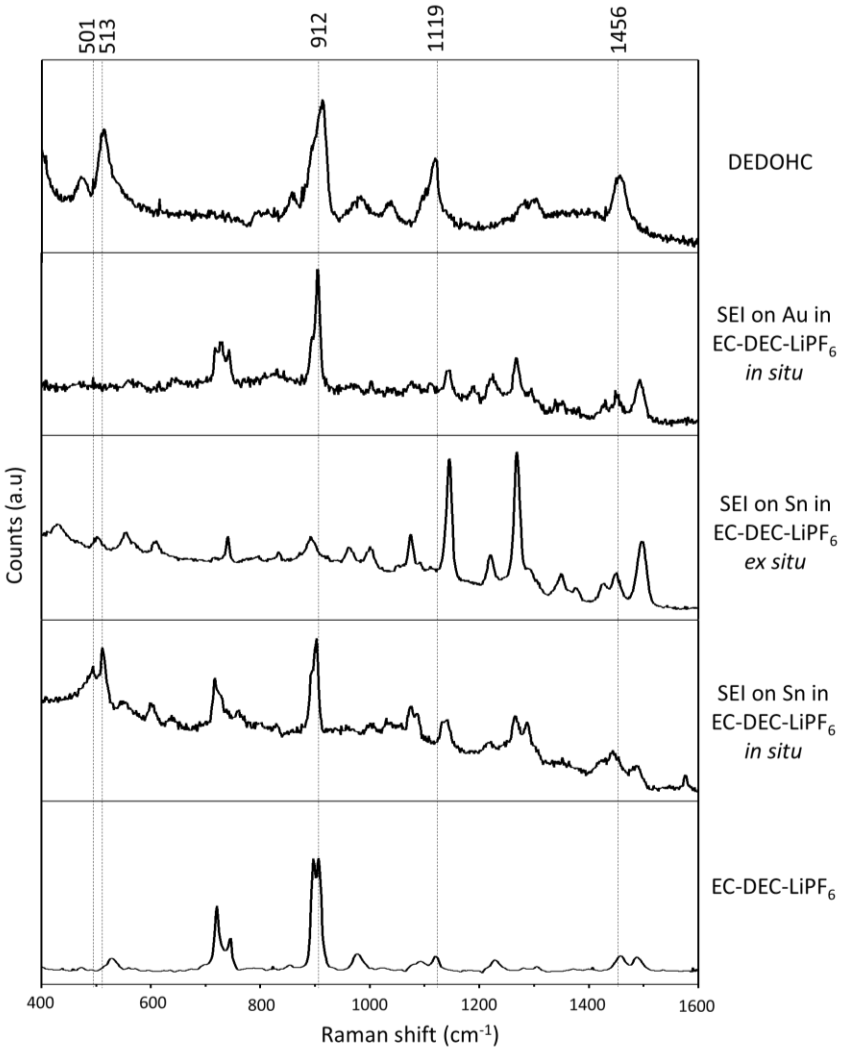

Figure S13: Comparison of the Raman spectra of the DEDOHC (diethyl 2,5-dioxahexane dicarboxylate) with the one of SEI formed on tin and gold anode (in situ and ex situ after 100mV polarization EC/DEC=50/50 (v/v), 1.0 M $LiPF_6$ electrolyte). All measurement were performed under Argon atmosphere at 785 nm.

SEI on tin in EC-DEC $LiPF_6$ electrolyte vs LEMC – As seen in **Figure S14**, most of the bands of the synthesized LEMC powder show spectra matching with band of the SEI obtained ex situ (LEMC is a stable specie not soluble in DEC). Thru this comparison, the main band of the SEI at 1266 cm^{-1} was assigned to LEMC (as one of the main product of the EC reduction).

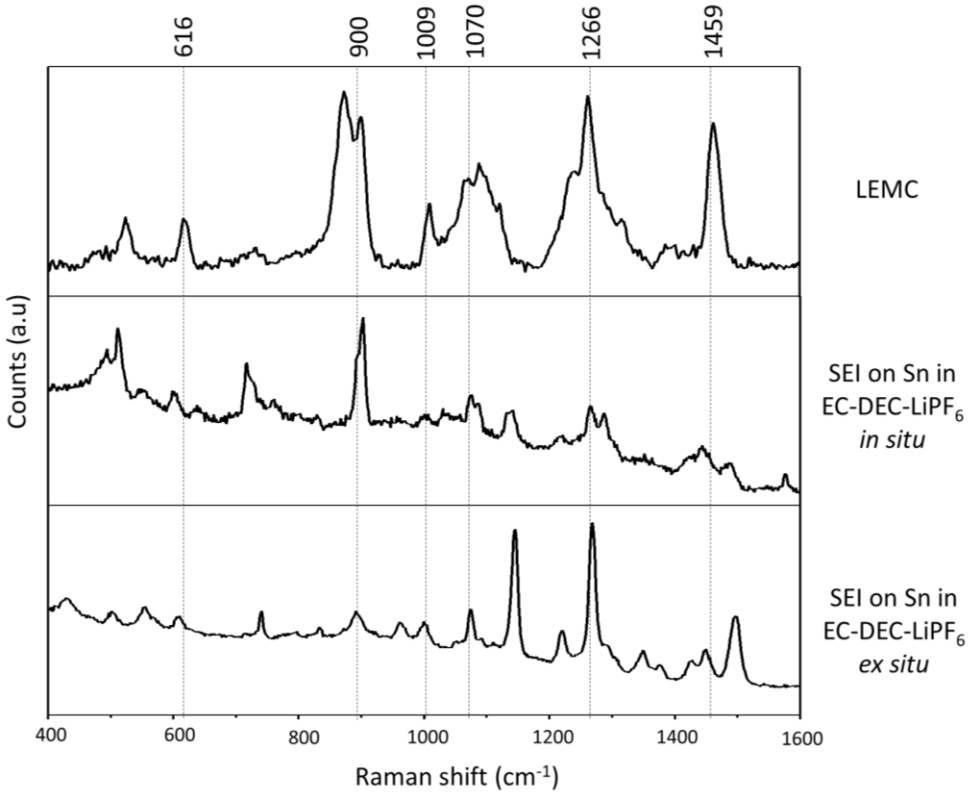

Figure S14: Comparison of the Raman spectra of the LEMC powder with the one of the SEI formed on tin (in situ and ex situ after 100mV polarization in EC/DEC=50/50 (v/v), 1.0 M $LiPF_6$ electrolyte). All measurement were performed under Argon atmosphere at 785 nm.

SEI on tin in EC-DEC LiPF6 electrolyte vs LEC – By comparing the Raman spectra of the SEI on tin with the one of synthesized LEC powder (**Figure S15**), different peaks of the SEI at 614, 888, 1009, 1275 and 1456 cm^{-1} could be attributed to the often reported LEC. However, the absence of Raman peak in the region of 1113 cm^{-1} in the SEI encourages us to be careful about the assignment of these bands.

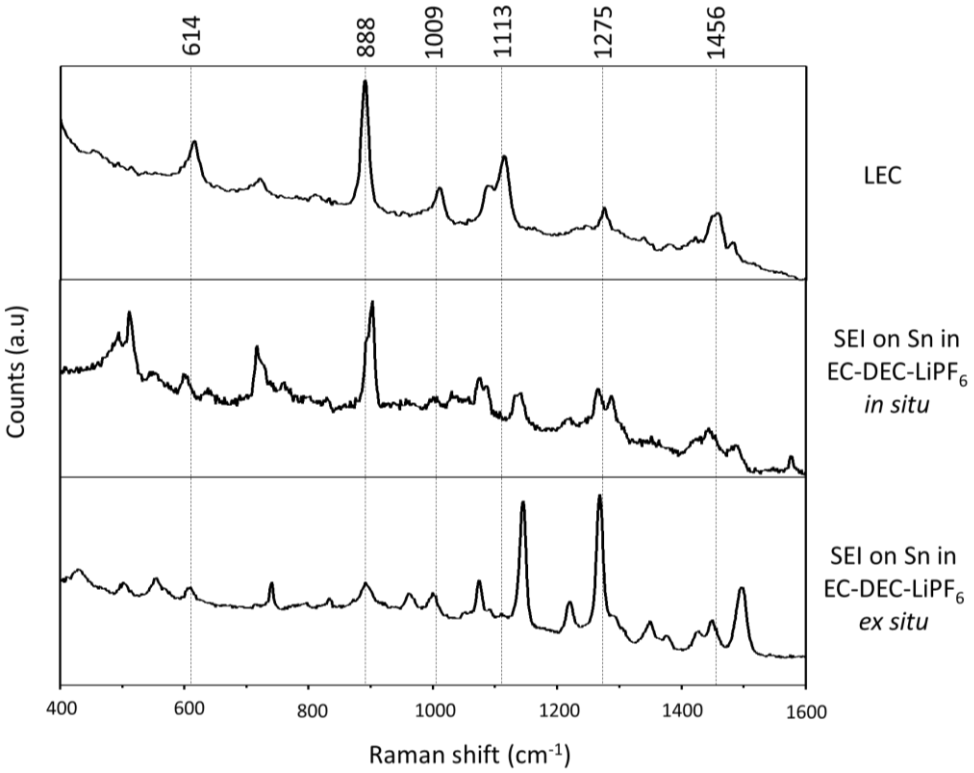

Figure S15: Comparison of the Raman spectra of the LEC powder with the one of the SEI formed on tin (in situ and ex situ after 100mV polarization in EC/DEC=50/50 (v/v), 1.0 M $LiPF_6$ electrolyte). All measurement were performed under Argon atmosphere at 785 nm.

SEI on tin in EC-DEC $LiPF_6$ electrolyte vs LEDC – By comparing the Raman spectra of the SEI on tin with the one of synthesized LEDC.2DMSO (**Figure S16**), no peaks of the SEI could be attributed to the often reported LEDC (main peak at 1090cm^{-1}).

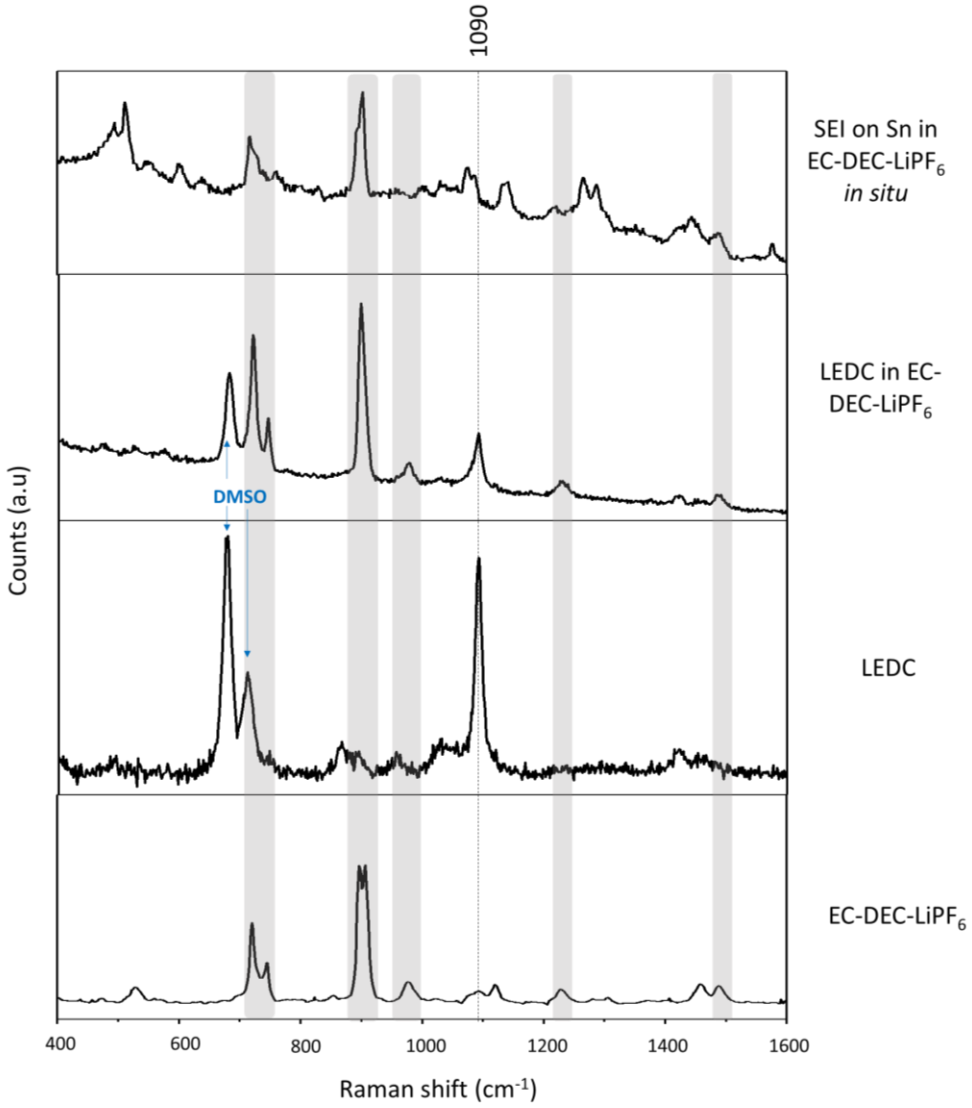

Figure S16 – Comparison of the Raman spectra of the SEI developed on tin in EC-DEC $LiPF_6$ (in situ SHINERS after 100mV polarization) with synthetic LEDC powder, soaked or not with EC-DEC 1.0 M $LiPF_6$ electrolyte. Note that the signature of the synthesis solvent DMSO is still observable (bands at 676 and 710 cm-1 marked with blue arrows). All measurement were performed under Argon atmosphere at 785 nm.

SEI on tin in PC $LiPF_6$ electrolyte vs LPDC– As seen in **Figure S17**, all the bands of the synthesized LPDC powder match with peaks of the SEI obtained in situ on tin in PC - 1.0 M $LiPF_6$ electrolyte. Thanks to this comparison, we can designate LPDC as one of the main product of PC reduction (instead of LEMC in EC based electrolyte). This attribution and the dynamic of formation of this specie will be discussed in a forthcoming dedicated publication.

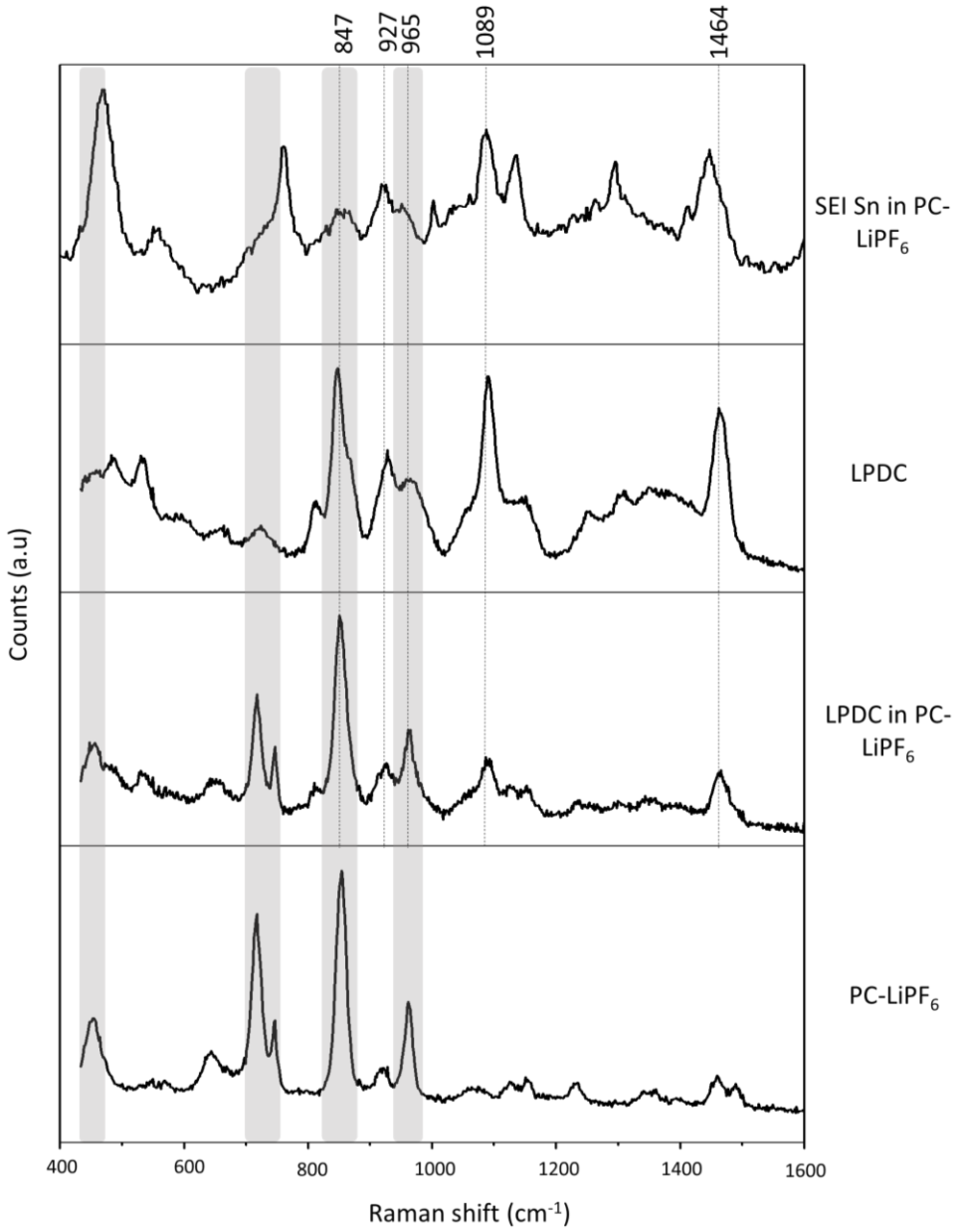

Figure S17: Comparison of the Raman spectra of the LPDC powder (alone or soaked with PC, 1.0 M $LiPF_6$ electrolyte) with the one of the SEI formed on tin (in situ after 100mV polarization in PC, 1.0 M $LiPF_6$ electrolyte). All measurement were performed under Argon atmosphere at 785 nm.

Supplemental References

1. Li, J.F., Tian, X.D., Li, S.B., Anema, J.R., Yang, Z.L., Ding, Y., Wu, Y.F., Zeng, Y.M., Chen, Q.Z., Ren, B., et al. (2013). Surface analysis using shell-isolated nanoparticle-enhanced Raman spectroscopy. Nature Protocols *8*, 52–65.

2. Cabo-Fernandez, L., Neale, A.R., Braga, F., Sazanovich, I.V., Kostecki, R., and Hardwick, L.J. (2019). Kerr gated Raman spectroscopy of $LiPF_6$ salt and $LiPF_6$ -based organic carbonate electrolyte for Li-ion batteries. Phys. Chem. Chem. Phys. *21*, 23833–23842.

3. Dedryvère, R., Gireaud, L., Grugeon, S., Laruelle, S., Tarascon, J.-M., and Gonbeau, D. (2005). Characterization of Lithium Alkyl Carbonates by X-ray Photoelectron Spectroscopy: Experimental and Theoretical Study. J. Phys. Chem. B *109*, 15868–15875.

4. Wang, L., Menakath, A., Han, F., Wang, Y., Zavalij, P.Y., Gaskell, K.J., Borodin, O., Iuga, D., Brown, S.P., Wang, C., et al. (2019). Identifying the components of the solid–electrolyte interphase in Li-ion batteries. Nat. Chem. *11*, 789–796.

5. Xu, K., Zhuang, G.V., Allen, J.L., Lee, U., Zhang, S.S., Ross, P.N., and Jow, T.R. (2006). Syntheses and Characterization of Lithium Alkyl Mono- and Dicarbonates as Components of Surface Films in Li-Ion Batteries. J. Phys. Chem. B *110*, 7708–7719.